

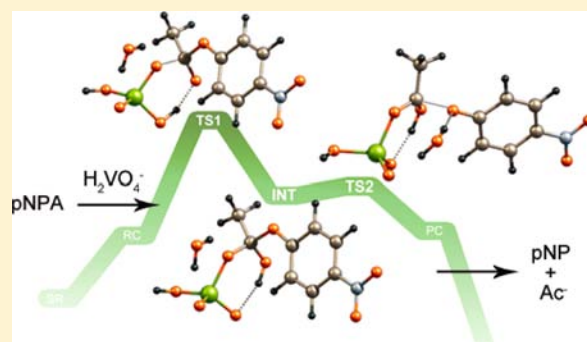
## Unraveling the Mechanisms of Carboxyl Ester Bond Hydrolysis Catalyzed by a Vanadate Anion

Tzvetan Mihaylov,\* Tatjana Parac-Vogt, and Kristine Pierloot

Chemistry Departement, University of Leuven, Celestijnenlaan 200F, B-3001 Leuven, Belgium

## Supporting Information

**ABSTRACT:** The mechanism of *p*-nitrophenyl acetate (pNPA) hydrolysis promoted by vanadate ions was investigated utilizing both density functional theory and ab initio methods. In accordance with experiments, suggesting pure hydrolytic ester bond cleavage involving a nucleophilic addition in the rate-limiting transition state, four possible  $B_{AC}2$  (acyl–oxygen bond cleavage) mode reaction pathways were modeled. Moreover, two alternative reaction modes were also considered. Geometry optimizations were carried out using B3LYP, BP86, and MPWB1K functionals, conjugated with a 6-31++G(d,p) basis set and a Stuttgart effective core potential (ECP) for the vanadium atom. Single-point calculations were performed utilizing M06, B3LYP-D, and BP86-D functionals as well as B2PLYP-D and MP2 methods with a 6-311++G(2d,2p) basis set (with and without ECP). To address bulk solvation effects, the universal solvation model (SMD) and the conductor-like polarizable continuum model were applied, using the parameters of water. All levels of theory predict the same reaction mechanism,  $B_{AC}2-1$ , as the lowest-energy pathway on the potential energy surface for pNPA hydrolysis catalyzed by the  $H_2VO_4^-$  ion in aqueous media. The  $B_{AC}2-1$  pathway passes through two transition states, the first associated with the nucleophilic addition of  $H_2VO_4^-$  and the second with the release of *p*-nitrophenoxide ion ( $pNP^-$ ), linked with a tetrahedral intermediate state. The intermediate structure is stabilized via protonation of the acyl oxygen atom by the vanadate and formation of an intramolecular hydrogen bond. The first and second barrier heights are 24.9 and 1.3 kcal/mol respectively, as calculated with the SMD-M06 approach. The theoretically predicted  $B_{AC}2-1$  mechanism is in good agreement with the experiment.



## INTRODUCTION

Nowadays the importance of vanadium in various biochemical processes is widely recognized. Several biological functions of vanadium have been described, including hormonal, cardiovascular, and antitumor activities.<sup>1</sup> The insulin-enhancing ability of vanadium compounds has also received growing interest over the past 2 decades.<sup>2–4</sup> A major area of vanadium biochemistry has been associated with monomeric vanadate ( $H_2VO_4^-/ HVO_4^{2-}$ ), which, because of its structural and electronic analogy with phosphate, often acts as a phosphate analogue in biological systems. However, over the last 2 decades, numerous studies have revealed that oligomeric forms of vanadate, such as tetrameric, pentameric, and decameric polyoxo forms, also possess important biological functions.<sup>5,6</sup> However, despite a number of studies pointing toward the biological importance of vanadate and its polyoxo forms, the molecular basis of this activity remains largely unexplored because these studies are often hindered by the complex solution chemistry of vanadate and the existence of equilibria with different polyoxoanions at physiological pH.<sup>7,8</sup>

While it has been mainly assumed that the mode of action of oxovanadates mostly depends on their structural features such as the charge and size of the species,<sup>9</sup> their reactivity toward biologically relevant substrates has been very scarcely explored.

Recent studies on the biological relevance of polyoxometalates revealed the unprecedented hydrolytic activity of oxovanadates toward several important classes of compounds such as phosphodiesteres, monophosphoesters,<sup>10,11</sup> and carboxylic esters.<sup>12</sup> In the case of phosphoesters, the kinetic experiments implicated polyoxovanadates as the hydrolytically active forms, and experimental evidence suggested that the origin of the phosphoesterase activity of oxovanadates lies in their high internal lability and their known ability to react with phosphate derivatives. However, experiments with a series of carboxylic esters identified monomeric vanadate as the kinetically active species. Both NMR and electron paramagnetic resonance (EPR) measurements showed no evidence of paramagnetic species, thus suggesting purely hydrolytic rather than oxidative carboxylic ester bond cleavage. The origin of the hydrolytic activity of vanadate was attributed to a combination of its nucleophilic nature and the ability to form a chelate complex with the reaction intermediate, which can lead to stabilization of the transition state. The observed esterase reactivity was suggested to play a role in some biological effects observed by vanadate in living systems.

Received: March 23, 2012

Published: September 6, 2012

Because of its importance in both biochemical processes and synthetic chemistry,<sup>13</sup> the hydrolysis of carboxylic acid esters is one of the most fundamental and extensively studied chemical reactions. Reactions involving acyl group transfer are widespread in nature, and there are many examples of hydrolysis of biologically related molecules such as esters (the metabolism of the neurotransmitter acetylcholine and the degradation of cocaine, for instance) or unsaturated fatty esters.<sup>14</sup> Normal ester bond cleavage by hydrolysis can occur rapidly in acidic or basic solution, but it is extremely slow in neutral solution for simple esters like ethyl acetate. The base-catalyzed hydrolysis of the majority of common esters occurs through nucleophilic attack of the hydroxide ion at the carbonyl carbon atom. A variety of experimental investigations have been reported about the ester hydrolysis catalyzed by alkaline solutions<sup>15–20</sup> and by hydroxide functions activated by an adjacent Lewis acid, mostly the Zn<sup>II</sup> ion.<sup>21–31</sup> However, most of the theoretical work is limited to ester hydrolysis catalyzed by alkaline solutions.<sup>32–38</sup> Common organic molecules such as imidazole and 2-methylimidazole, various substituted pyridines, and several enzymes (e.g., chymotrypsin, acetylcholinesterase, dehydrogenase, and ribonuclease) have been exploited as catalysts.<sup>13,14,39–41</sup> A variety of metal complexes including cobalt, zinc, copper, and many lanthanides have been found to be effective at promoting hydrolysis.<sup>42</sup> Previous studies have suggested that metal complexes are effective catalysts because of the possibility of Lewis acid activation, formation of an intramolecular nucleophile at physiological pH, or stabilization of the leaving group.<sup>43,44</sup> Several oxanions, including MoO<sub>4</sub><sup>2-</sup>, WO<sub>4</sub><sup>2-</sup>, and CrO<sub>4</sub><sup>2-</sup>, were also tested for their ability to cleave carboxylic acid esters; however, only CrO<sub>4</sub><sup>2-</sup> and MoO<sub>4</sub><sup>2-</sup> were shown to be hydrolytically active.<sup>45–47</sup>

In the case of the vanadate-promoted hydrolysis of carboxylic acid esters such as *p*-nitrophenyl acetate (pNPA), *p*-nitrophenyl butyrate (pNPB), and *p*-nitrophenyl trimethyl acetate (pNPTA), both general base and nucleophilic attack mechanisms are plausible. The solvent deuterium isotope effect for pNPA hydrolysis in the presence of vanadate is 1.27, suggesting a nucleophilic mechanism.<sup>12</sup> In addition, the interaction with vanadium can lead to stabilization of the transition state by forming a V–O bond with the incipient oxanion of the ester carbonyl (Figure 1a), similar to the previously proposed MO<sub>4</sub><sup>2-</sup> (M = Cr, Mo)-promoted hydrolysis of carboxylic esters (Figure 1b).<sup>47</sup> The slower reaction rate observed for pNPB and pNPTA (with respect to pNPA) is in agreement with the formation of such a chelate because bulky leaving groups on these substrates sterically hinder efficient chelation, which, in turn, results in slower hydrolysis of the ester bond. The observed decrease of the rate constant of cleavage upon increases in the amounts of acetonitrile in the water solutions (decreases of the dielectric constant of the solvent mixture) could be taken as evidence for the involvement of charged species in the reaction intermediate.<sup>12</sup> However, despite the experimental evidence, the molecular mechanism of this reaction still remains unclear. Considering the biological importance of vanadate, understanding its reactivity toward biologically relevant model systems under physiological conditions is of ultimate importance.

In order to gain deeper insight into the catalytic role of oxovanadate in ester hydrolysis reactions, we examine in this study the pure hydrolytic cleavage of the pNPA ester bond promoted by H<sub>2</sub>VO<sub>4</sub><sup>-</sup> in aqueous media. A detailed picture of

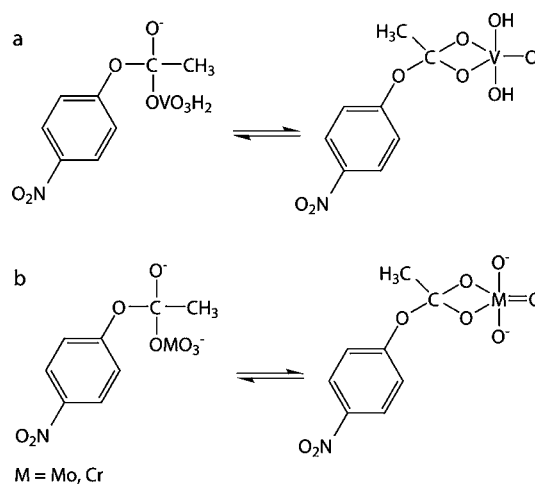


**Figure 1.** Possible formation of a chelate, which could stabilize the tetrahedral addition intermediate in oxometalate-catalyzed ester hydrolysis.

the possible reaction mechanisms by means of different density functional theory (DFT) and ab initio methods is provided, taking into account the experimental data available. The calculated reaction pathways are analyzed in terms of transition-state theory, and the most probable mechanism is proposed.

## ■ COMPUTATIONAL DETAILS

All geometric structures of the reactants, intermediates, transition states, and products in the hydrolysis pathways were optimized in the gas phase without constraints using the hybrid DFT method B3LYP.<sup>48–50</sup> A combination of the LANL2DZ valence double- $\zeta$  basis set with an effective core potential (ECP)<sup>51,52</sup> for the vanadium atom and the 6-31+G(d,p) basis set for all other atoms was employed (this basis set will be further denoted as B1). To confirm the character of all first-order saddle points and local minima on the potential energy surface (PES), vibrational frequency calculations were carried out. Intrinsic reaction coordinate (IRC) calculations were performed at the same theoretical level to verify the expected connections between the first-order saddle points and local minima on the PES. Subsequently, all B3LYP/B1 structures were refined with the same functional but using a more extended basis set combination B2, consisting of the relativistic Stuttgart pseudopotential (SDD, describing 10 core electrons) with the appropriate contracted basis set (8s7p6d1f)/[6s5p3d1f]<sup>53</sup> for the vanadium atom, combined with 6-31++G(d,p) basis sets for the other atoms. The B3LYP DFT method, in combination with Stuttgart pseudopotentials and 6-31++G(d,p) basis sets, is a quite reasonable approach for the investigation of the reactivity and mechanism of reactions involving transition-metal complexes, taking into account the low computational cost of this method and general good agreement with the experimental data. Moreover, the 6-31++G(d,p) basis sets were previously found to be large enough for an accurate description of the alkaline hydrolysis of carboxylic acid esters.<sup>36</sup> The B3LYP functional is known to provide accurate predictions of equilibrium geometries and energies for minima. However, it gives a less accurate prediction of transition-state geometries.<sup>54</sup> Therefore, in addition, optimizations were also performed with the pure gradient-corrected (generalized gradient approximation, GGA) functional BP86<sup>49,55</sup> and the hybrid meta-GGA functional MPWB1K<sup>56</sup> using the same basis B2. The second functional was chosen because of its accurate performance with respect to the barrier heights of a benchmark set of non-hydrogen-transfer reactions, including reactions of nucleophilic substitution.<sup>57</sup> Moreover, MPWB1K has proven to be among the most accurate functionals for calculation of the activation and reaction energies of phosphodiester bond hydrolysis.<sup>58</sup> Because of our intention to expand

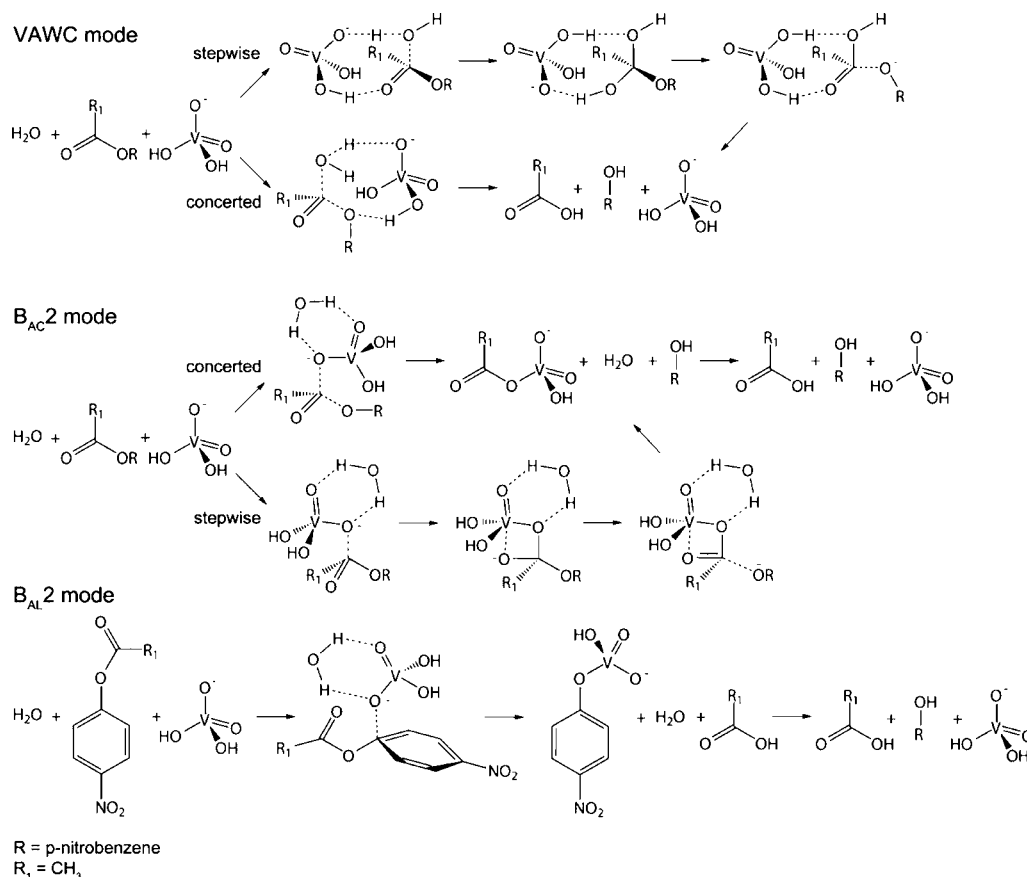


**Figure 2.** Schematic presentation of the VAWC B<sub>AC</sub>2, and B<sub>AL</sub>2 reaction modes of pNPA ester bond cleavage catalyzed by H<sub>2</sub>VO<sub>4</sub><sup>-</sup>.

this research to the investigation of the catalytic role of polyoxovanadate ions for phosphodiester bond cleavage, it is advantageous to test the performance of MPWB1K in this study. The optimized geometries for each species at all theoretical levels are very similar and qualitatively consistent with respect to the presence of local minima or first-order saddle points on the corresponding PESs. The qualitative consistency of the results calculated at various levels supports the reliability of the geometry optimizations in this study.

To assess the basis set effect and the influence of the metal ECP on the relative energies of the stationary points, single-point calculations were performed utilizing basis set combination B3, consisting of SDD ECP for vanadium and 6-311++G(2d,2p) for the other atoms, and B4, 6-311++G(2d,2p) for all atoms. Moreover, B3LYP/B2 geometries were used in single-point computations with basis set B4 and the M06 functional, which is recommended by the Truhlar group for transition-metal thermochemistry and problems involving the rearrangement of both organic and transition-metal bonds.<sup>59,60</sup> It is known that DFT methods usually underestimate reaction barrier heights,<sup>59,61</sup> but highly accurate *ab initio* methods such as CCSD(T) and QCISD(T) with appropriate basis sets require a too large computational resource and are still inaccessible for our systems. Hence, to check the reliability of the DFT calculations described above, the post Hartree–Fock MP2 method and the double-hybrid density functional (that adds nonlocal electron correlation effects to a standard hybrid functional by second-order perturbation theory) B2PLYP-D<sup>62,63</sup> with long-range dispersion correction were employed. The accuracy of B2PLYP-D for main-group thermochemistry, kinetics, and noncovalent interactions has been demonstrated previously.<sup>64</sup> The influence of the dispersion interactions on the reaction profiles was examined by performing B3LYP-D/B4 and BP86-D/B4 single-point calculations.

To address bulk solvation effects, the universal solvation model (SMD)<sup>65</sup> (where “universal” denotes its applicability to any charged or uncharged solute in any solvent or liquid medium) and the conductor-like polarizable continuum model (CPCM)<sup>66,67</sup> were applied, using

the parameters of water. Because in this work all stationary-point structures along the hydrolysis reaction are negatively charged, it is important to select an appropriate approach for calculation of the aqueous solvation free energies for anion molecules. For the SMD calculations, the HF/6-31G(d) level has been chosen on the basis of the results presented in the original SMD paper.<sup>65</sup> In CPCM, the choice of cavities is important because the computed energies and properties depend on the cavity size. Because some of the transition states studied here involve a proton in flight, the choice of cavity is constrained by the requirement to use atomic radii with explicit hydrogen atoms. Taking into account a benchmark study pointing out the combination of Pauling cavities and the HF/6-31+G(d) level as the most appropriate for calculation of the solvation free energies of anion molecules,<sup>68</sup> we make use of this approach. In both cases, SMD and CPCM, the vanadium electrons were described with a LANL2DZ valence double- $\zeta$  basis set with ECP. Single-point SMD and CPCM calculations were performed on the B3LYP/B2 gas-phase-optimized geometries. In addition, the SMD-B3LYP/6-31G(d) approach as well as a few more CPCM variants combined with HF and B3LYP methods was examined [see the Supporting Information (SI) for details].

The free-energy change of the reacting system in aqueous phase  $\Delta G_{aq}$  is estimated by adding the free-energy change of solvation ( $\Delta\Delta G_{solv}$ ) to the computed ideal gas-phase relative free energies ( $\Delta G^\circ$ ). It should be emphasized that the ideal gas-phase model intrinsically overestimates the entropic contributions because it ignores the suppression effects of solvent on the rotational and translational freedoms of the reactants.<sup>69</sup> The accurate prediction of entropies in solution is still a challenge for computational chemistry, and no standard approach is currently available.<sup>70–72</sup> Pratt et al. proposed to correct the overestimation of the entropic contributions by artificially elevating the reaction pressure from 1 to 1354 atm.<sup>73</sup> According to their approach, an additional 4.27 kcal/mol free-energy correction applies to each component change for a reaction at 298.15 K and 1 atm [i.e., a reaction from  $m$  to  $n$  components has an additional free-

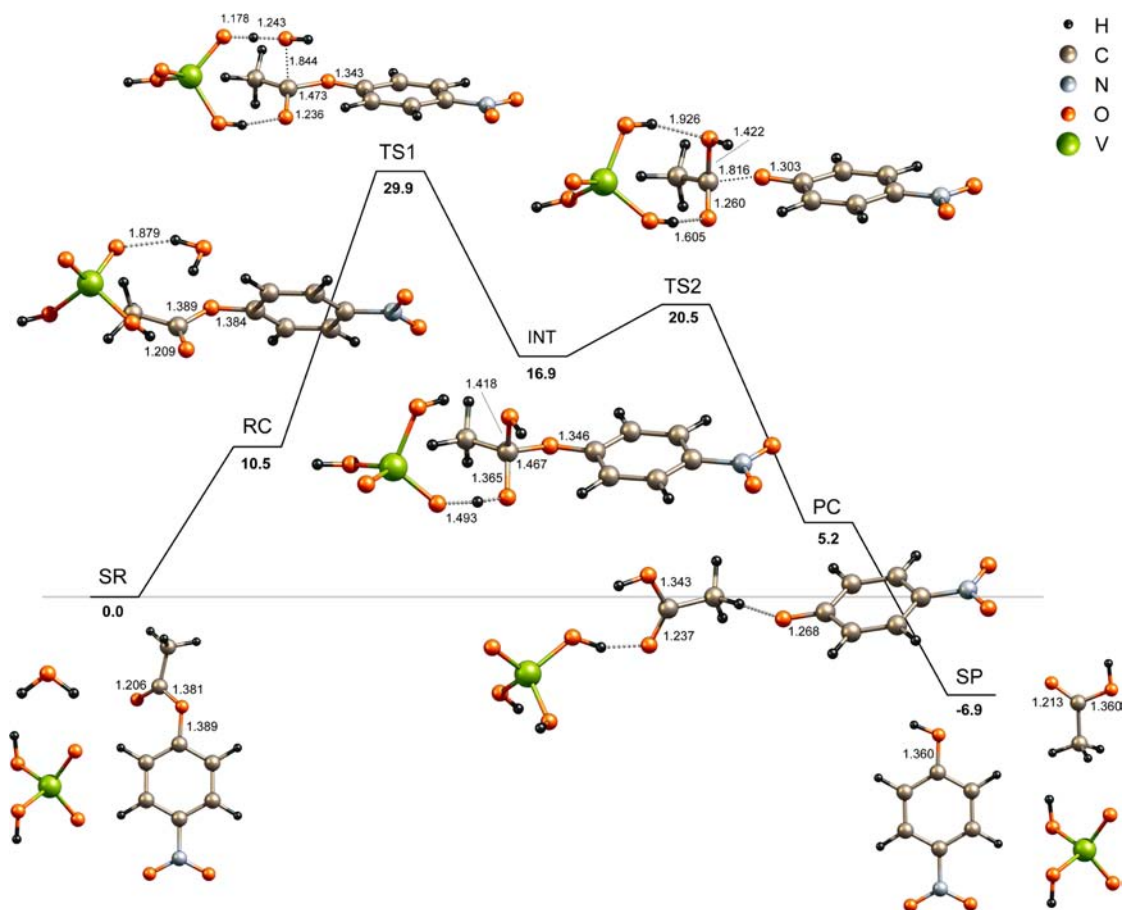


**Figure 3.** Reaction pathway for stepwise hydrolysis of pNPA via the VAWC-1 mechanism. Relevant interatomic distances optimized in the gas phase at the B3LYP/B2 level of theory are indicated in angstroms. Relative free energies in the aqueous phase calculated at the SMD-M06/B4//B3LYP/B2 level of theory are given in kilocalories per mole.

energy correction of  $(n - m) \times 4.27$  kcal/mol]. Thus, for our termolecular reactions, this means a lowering of the reaction barriers by 8.5 kcal/mol. Unless otherwise noted, our discussion of the reaction profiles below will be based on the free energies obtained after adjustment for the concentration in the liquid ( $p = 1354$  atm).

For the BP86 and MPWB1K single-point calculations, free-energy corrections derived from the BP86/B2 and MPWB1K/B2 levels were used. For the rest of the methods, corrections to the free energy were taken from B3LYP/B2 thermochemistry.

All calculations were performed with the *Gaussian 03*<sup>74</sup> and *Gaussian 09*<sup>75</sup> suites of programs.

## RESULTS AND DISCUSSION

As is well-known, ester hydrolysis ( $R'COOR + H_2O \rightarrow R'COOH + ROH$ ) involves cleavage of either the acyl–oxygen ( $B_{AC2}$  mode of hydrolysis) or alkyl–oxygen ( $B_{AL2}$  mode of hydrolysis) bond.<sup>76</sup> Both types of cleavage are experimentally observed with both acid and base catalysts, and the result is a rich array of possible reaction mechanisms. The base-catalyzed hydrolysis of the majority of common alkyl esters occurs as a two-step mechanism consisting of the formation of a tetrahedral intermediate (first step), followed by decomposition of the tetrahedral intermediate into products (second step). On the other hand, isotopic labeling studies<sup>77</sup> and *ab initio* calculations<sup>78</sup> have suggested that base-catalyzed hydrolysis of pNPA occurs through a concerted process. In the  $H_2VO_4^-$ -catalyzed ester hydrolysis of pNPA in a neutral water solution, the  $H_2VO_4^-$  ion could most likely serve as a nucleophilic

catalyst. However, an alternative mechanism, in which the  $H_2VO_4^-$  ion rather acts as a general base, assisting the addition of a water molecule, is also plausible. A schematic presentation of the reaction modes considered in this study is given in Figure 2. Because a nucleophilic attack can be accomplished either at the acyl or alkyl carbon atom, both the  $B_{AC2}$  and  $B_{AL2}$  modes of reaction are considered in this work. For the  $B_{AC2}$  mode hydrolysis, both a stepwise and a concerted pathway are modeled. An alternative catalytic pathway (general base activity) is inspired by the solution chemistry of the  $H_2VO_4^-$  ion. DFT-based Carr–Parrinello molecular dynamics studies have suggested that the first solvation shell of  $H_2VO_4^-$  consists of around eight water molecules<sup>79</sup> and that frequent proton exchange between the solute and solvent might take place in solution.<sup>80</sup> Therefore, the third kind of reactions modeled in this study is based on the assumption that, in the solvated molecular complex formed by the reactants ( $H_2VO_4^-$ , pNPA, and  $H_2O$ ), simultaneous vanadate-induced deprotonation of a water molecule and attack of the resulting hydroxyl ion at the acyl carbon atom of pNPA might occur. This mode of catalytic action will further be denoted as vanadate-assisted water catalysis (VAWC) and is also shown in Figure 2. It should be mentioned that Figure 2 presents only a general picture of the reaction modes considered, but the variety of the molecular arrangements give rise to a number of individual pathways for every reaction mode.

Our attempts to model possible reactions where the vanadate ion acts as a general base led to the identification of three

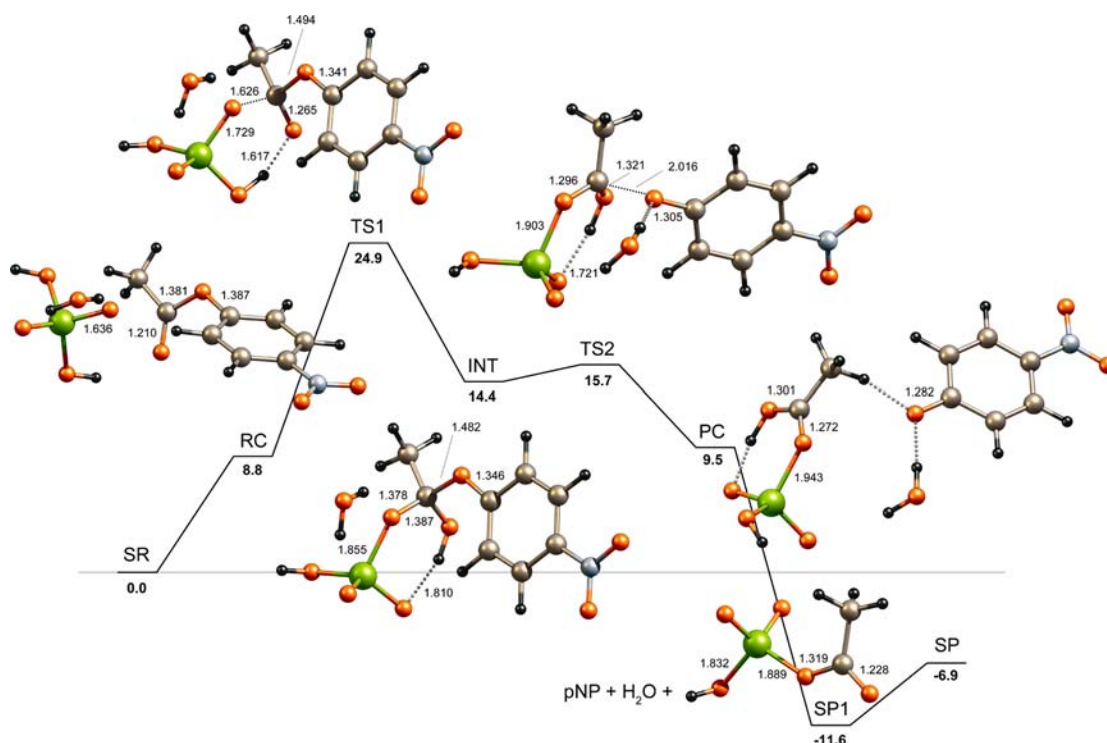


**Figure 4.** Reaction pathway for stepwise hydrolysis of pNPA via the  $B_{AC}2-1$  mechanism. Relevant interatomic distances optimized in the gas phase at the B3LYP/B2 level of theory are indicated in angstroms. Relative free energies in the aqueous phase calculated at the SMD-M06/B4//B3LYP/B2 level of theory are given in kilocalories per mole.

different pathways denoted as VAWC-1, VAWC-2, and VAWC-3. In probing the nucleophilic catalytic activity of the vanadate ions toward pNPA, four individual reaction pathways of the  $B_{AC}2$  mode ( $B_{AC}2-1$ ,  $B_{AC}2-2$ ,  $B_{AC}2-3$ , and  $B_{AC}2-4$ ) and two pathways of the  $B_{AL}2$  mode ( $B_{AL}2-1$  and  $B_{AL}2-2$ ) were modeled. It should be emphasized here that there is a vast conformational freedom in the reacting system. We do not want to pretend that all possible molecular arrangements were examined, but we do think that the most obvious ones are included in our study. It is worth noting that the results obtained with the different approaches in this work are qualitatively consistent (with small exceptions discussed in the SI), and VAWC-1,  $B_{AC}2-1$ , and  $B_{AL}2-1$  are pointed out as the lowest-energy paths on the PES for the VAWC,  $B_{AC}2$ , and  $B_{AL}2$  modes, respectively. Among all model reactions,  $B_{AC}2-1$  has the lowest activation energy. We also found that the rate-limiting barrier height of this reaction, calculated at the SMD-M06/B4//B3LYP/B2 level, is in the best agreement with the experimentally estimated activation Gibbs function for vanadate-promoted pNPA hydrolysis.<sup>12</sup> Given that above and to avoid the extensive and tedious description of all reaction pathways accompanied with a large amount of numerical data (from different levels of theory), our discussion below will be focused mainly on the VAWC-1,  $B_{AC}2-1$ , and  $B_{AL}2-1$  paths as calculated at the SMD-M06/B4//B3LYP/B2 level of theory. The rest of the reaction pathways along with our analysis about the performance of the different quantum chemical methods, solvation models, and basis sets are presented in the SI.

**Hydrolysis of pNPA via a VAWC Mode: VAWC-1 Pathway.** pNPA hydrolysis via the VAWC-1 pathway occurs through a two-step mechanism. As depicted in Figure 3, the first transition state (TS1) connects a complex formed by the reactants, RC (pNPA,  $H_2O$ , and  $H_2VO_4^-$ ), with a tetrahedral

intermediate, INT. In TS1, the vanadate ion acts in a 2-fold manner. On the one hand, a partial proton transfer occurs from the attacking water molecule to a vanadate oxygen atom. On the other hand, one of the vanadate hydroxyl groups becomes hydrogen-bonded to the carbonyl oxygen atom of pNPA ( $V-OH \cdots O=C$ ). This produces additional polarization of the  $C=O$  bond, thus increasing the positive charge on the acyl carbon atom and facilitating attack by the partially deprotonated water molecule. According to the IRC calculations, the transfer of a proton to the vanadate oxygen atom and the formation of the  $O-C$  bond between the resultant hydroxyl ion and acyl carbon atom proceed simultaneously. During formation of the intermediate, the proton involved in the  $V-OH \cdots O=C$  hydrogen bond moves to the acyl oxygen atom without an energy barrier. Such a barrierless proton transfer is the hallmark of a short strong hydrogen bond. INT is connected to the product complex (PC) through a second transition state (TS2) associated with the release of the *p*-nitrophenoxide ion ( $pNP^-$ ). The formation of TS2 is preceded by a reverse proton transfer to the vanadate. The calculated distance between the oxygen of the attacking water and the acyl carbon atom in TS1 is 1.844 Å, which is much shorter than the  $O \cdots C$  distance reported for the base-catalyzed hydrolysis of pNPA (2.20 Å).<sup>78</sup> In the TS2 structure, the ester bond is stretched by 0.349 Å compared to INT. To conserve the number of charged species along the reaction, the acetic acid in SP is considered in its protonated form (HAc). The energy gain of the overall hydrolysis reaction is thus estimated at  $-6.9$  kcal/mol. The effect of HAc dissociation on the reaction energy is discussed further, in the Reaction Products section.

The calculations predict a higher relative energy of TS1 with respect to TS2, pointing out that the first reaction step should be the rate-limiting step for pNPA hydrolysis via the VAWC-1

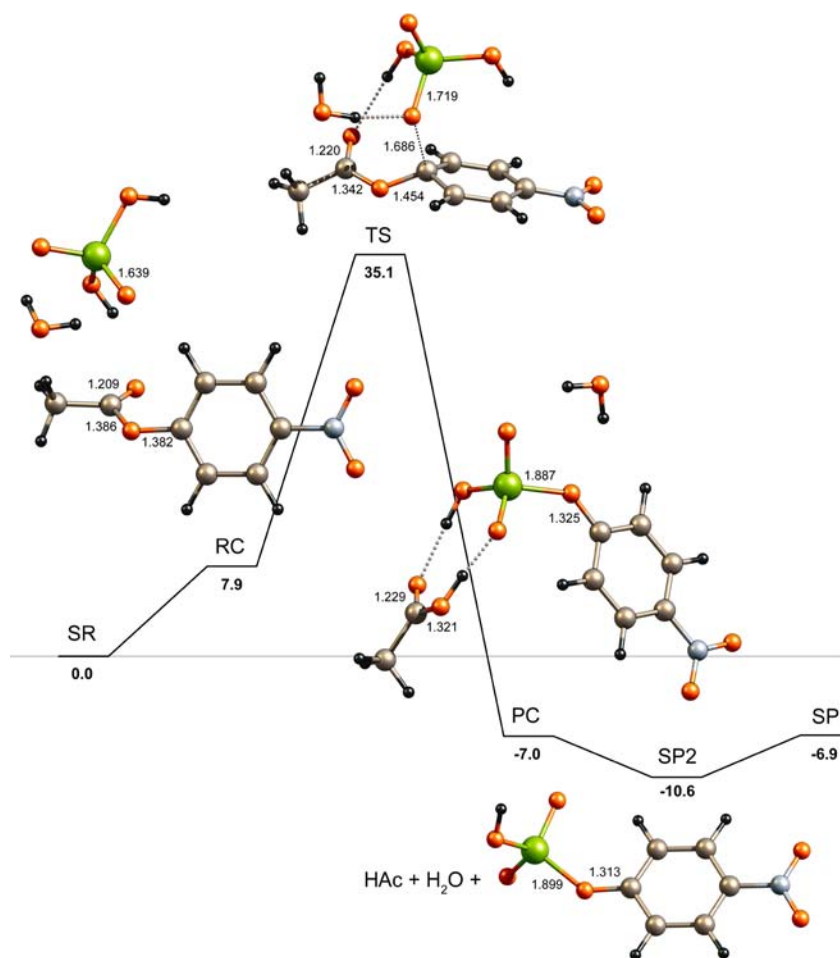


**Figure 5.** Reaction pathway for the concerted hydrolysis of pNPA via the  $B_{AL}2-1$  mechanism. Relevant interatomic distances optimized in the gas phase at the B3LYP/B2 level of theory are indicated in angstroms. Relative free energies in the aqueous phase calculated at the SMD-M06/B4//B3LYP/B2 level of theory are given in kilocalories per mole.

route. The first barrier height is estimated at 29.9 kcal/mol, and the second one, corresponding to the  $pNP^-$  departure, is estimated at 3.6 kcal/mol (INT  $\rightarrow$  TS2).

Additional thermodynamic data calculated at various levels of theory may be found in Tables S1 and S2, given in the SI.

#### Hydrolysis of pNPA via a $B_{AC}2$ Mode: $B_{AC}2-1$ Pathway.

Following previous suggestions<sup>12</sup> that the hydrolytic activity of vanadate is most likely underlied by its nucleophilic nature as well as by its ability to stabilize a reaction intermediate through chelation, different variants of the  $B_{AC}2$  mode of catalysis were explored. For instance, the  $B_{AC}2-2$  pathway is modeled as a one-step concerted mechanism, whereas  $B_{AC}2-3$  and  $B_{AC}2-4$  are designed as stepwise mechanisms where the first and second transition states are connected through an intermediate five-coordinated vanadium chelate complex (see the SI), as was proposed by experimentalists. The lowest-energy pathway of hydrolysis,  $B_{AC}2-1$ , is a stepwise process, shown in Figure 4. It passes through two transition states, the first (TS1) associated with the nucleophilic addition of  $H_2VO_4^-$  at the acyl carbon atom to form a tetrahedral intermediate (INT) and the second (TS2) with the release of  $pNP^-$  from this intermediate. In TS1, a vanadate oxygen atom approaches the acyl carbon atom to within 1.626 Å and the adjacent acyl oxygen atom forms a short strong hydrogen bond with one of the vanadate OH groups ( $R_{VOH\cdots O=C} = 1.617$  Å). This hydrogen bonding polarizes the C=O bond and facilitates the nucleophilic addition. The

energy lowering from TS1 to INT is accompanied by proton transfer along the  $V-OH\cdots O=C$  hydrogen bond. The relative free energy in solution of TS1 is calculated at 24.9 kcal/mol, which is 9.2 kcal/mol higher compared to that of TS2. As such, the first step of the addition should be considered as the bottleneck of the overall process of pNPA hydrolysis via a  $B_{AC}2-1$  pathway. Because of the structural similarity between INT and TS2, the activation energy required for the release of  $pNP^-$  is very small, estimated at 1.3 kcal/mol (INT  $\rightarrow$  TS2), in agreement with Hammond's postulate.

Unlike the INT structures of  $B_{AC}2-3$  and  $B_{AC}2-4$  (see the SI), the tetrahedral intermediate of the  $B_{AC}2-1$  pathway is stabilized through protonation of the negatively charged acyl oxygen atom and the formation of a  $V-O\cdots HO-C(\text{acyl})$  hydrogen bond rather than through coordination of the acyl oxygen atom to vanadium, giving rise to a chelate complex.

As a result from the nucleophilic addition of the vanadate at the ester acyl carbon atom, the  $B_{AC}2$  mode reactions are accompanied by the formation of vanadate acetyl ester (SP1, depicted in Figure 4). The aqueous free energy of SP1 is calculated as considerably lower than that of SP, thus predicting the formation of vanadate acetyl ester as the major compound of the overall hydrolysis. This contradicts the experiment, where only pNP and  $Ac^-$  were detected as products, but could be explained by taking into account the HAc dissociation energy, as discussed below (Reaction Products section).

Thermodynamic data for the  $B_{AC}2-1$  pathway, calculated at all levels of theory utilized in this work, are given in Tables S3 and S4 in the SI.

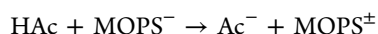
**Hydrolysis of pNPA via a  $B_{AL}2$  Mode: the  $B_{AL}2-1$  Pathway.** Alkaline ester hydrolysis via the  $B_{AL}2$  mode leads to the same reaction products as the  $B_{AC}2$  process but is essentially an  $S_N2$  substitution with a carboxylate leaving group.<sup>76</sup> Compared to  $B_{AC}2$ ,  $B_{AL}2$  is a less common mode of ester hydrolysis, but in some cases, it may contribute significantly to the reaction output.

The  $B_{AL}2-1$  pathway of the vanadate-promoted pNPA hydrolysis passes through a transition state, associated with an energy barrier estimated at 35.1 kcal/mol (Figure 5). In this transition state, the phenyl–oxygen bond is distorted by around 38° out of the phenyl ring plane. A vanadate oxygen atom approaches the alkyl carbon atom to within 1.686 Å, attacking at an angle (with respect to the pNP ring) of 121°. The products of the transition state decomposition (denoted as SP2) are vanadate *p*-nitrophenyl ester (pNP-VO<sub>3</sub>H<sup>-</sup>), acetic acid, and water. In the preceding product complex (PC), these three moieties are hydrogen-bonded. On the basis of the calculated free energies for SP2 and SP, we predict the formation of *p*-nitrophenyl vanadate as a major product of the hydrolysis process (see the next section).

Calculated thermodynamic data for the  $B_{AC}2-1$  pathway are given in Tables S5 and S6 in the SI.

**Reaction Products.** As was shown above, along with the expected products of pNPA hydrolysis (pNP and Ac<sup>-</sup>), our models also predict formation of acetyl and *p*-nitrophenyl vanadates. It is known from the literature that H<sub>2</sub>VO<sub>4</sub><sup>-</sup> may interact with acetic acid to form mixed acid anhydrides, i.e., mainly bis(acetate)vanadate.<sup>81</sup> Vanadate esters of various phenyl derivatives, including pNP, were also reported.<sup>82</sup> In acetone–water mixtures, vanadate, in fact, spontaneously reacts with phenols to form phenyl vanadates. The formation of such compounds in the reaction conditions where vanadate-promoted ester hydrolysis takes place was checked by means of <sup>13</sup>C NMR. The spectra of pNP and Ac<sup>-</sup> recorded in the absence and presence of vanadate exhibit significant shifts, indicating that interactions took place in solution.<sup>12</sup>

According to the calculations (see the  $B_{AC}2-1$  pathway in Figure 4), the relative free energy in solution of SP1 (Ac-VO<sub>3</sub>H<sup>-</sup>, pNP, and water) is lower than that of SP (pNP, HAc, and H<sub>2</sub>VO<sub>4</sub><sup>-</sup>) by 4.7 kcal/mol, thus predicting the predominant formation of Ac-VO<sub>3</sub>H<sup>-</sup> from its parent compounds HAc and H<sub>2</sub>VO<sub>4</sub><sup>-</sup>. To keep the number of charged species constant along the reaction, the HAc form has been chosen in our models, whereas in the experimental reaction conditions (pH = 7.4), this molecule mainly exists in its deprotonated form (Ac<sup>-</sup>). It is known that the overall reaction enthalpy change for pNPA hydrolysis is dominated by the enthalpy change corresponding to the buffer protonation.<sup>83</sup> For vanadate-promoted pNPA hydrolysis, the pH of the reaction mixture is kept fixed by means of a 3-(*N*-morpholino)propanesulfonic acid (MOPS) buffer.<sup>12</sup> The reaction



was found to be exergonic by -4.2 kcal/mol at the SMD-M06/B4//B3LYP/B2 level. Adding this value to the  $\Delta G_{aq}$  value of SP (-6.9 kcal/mol), we obtain -11.1 kcal/mol in total, which is very close to the  $\Delta G_{aq}$  value of SP1 (-11.6 kcal/mol). Thus, taking into account the HAc–MOPS<sup>-</sup> interaction, the SP → SP1 conversion could be considered as an isoergonic process

(SP and SP1 are in equilibrium). However, the same argument cannot be used to explain the discrepancy between theory and experiment in the case of the  $B_{AL}2-1$  pathway (Figure 5), where the formation of SP2 (pNP-VO<sub>3</sub>H<sup>-</sup>, HAc, and water) rather than SP (pNP, HAc, and H<sub>2</sub>VO<sub>4</sub><sup>-</sup>) is theoretically predicted but where now both SP and SP2 contain HAc in the same form. Obviously, other factors that might originate from either the theoretical approach or the complex equilibrium in solution (where a number of conditions could play a decisive role, e.g., temperature, concentration, ionic strength, etc.) have to be taken into account. To the best of our knowledge, the formation/hydrolysis mechanism of both phenyl vanadates and vanadate anhydrides like Ac-VO<sub>3</sub>H<sup>-</sup> is not known,<sup>84</sup> and its elucidation, or how SP, SP1, and SP2 convert to each other, goes beyond the main goals of this study.

**Analysis of the Reaction Pathways.** In this study, we consider three different modes of reaction mechanisms of pNPA hydrolysis with a different nature of the rate-limiting transition states. The VAWC pathways involve transition states associated with a proton in flight, whereas  $B_{AC}2$  and  $B_{AL}2$  involve transition states associated with both nucleophilic addition and substitution without water splitting. Not surprisingly, the transition state energies predicted at different levels of theory vary in a broad range, but all DFT results are qualitatively consistent. A more thorough discussion of the different theoretical approaches and their performances is documented in the SI. Here, we will highlight only some general outcomes. For the stepwise mechanisms, the first addition step always has the highest-energy requirement and is the bottleneck for the overall process of hydrolysis. A comparison between the  $\Delta G_{aq}$  values for the reaction barriers reveals that the  $B_{AL}2$  pathways are unambiguously less likely than  $B_{AC}2$  (as is found for alkaline hydrolysis of the common esters)<sup>38</sup> and VAWC as well. The calculations clearly predict  $B_{AC}2-1$ , VAWC-1, and  $B_{AL}2-1$  as the lowest-energy reaction pathways on the PES in solution for respectively the  $B_{AC}2$ , VAWC, and  $B_{AL}2$  reaction modes. Thermodynamic data for their rate-limiting transition states are summarized in Table 1.

**Table 1. Ideal-Gas and Aqueous Reaction Thermochemistries (kcal/mol) of the Rate-Limiting Transition States of pNPA Hydrolysis Calculated at the M06/B4//B3LYP/B2 Level of Theory and with an SMD Solvation Model**

mechanism	$\Delta H^\circ$	$\Delta G^\circ$	$\Delta G^a$	$\Delta \Delta G_{\text{solv}}$	$\Delta G_{\text{aq}}^b$	$\Delta G_{\text{exp}}^\ddagger$ [ $\Delta H_{\text{exp}}^\ddagger$ ] <sup>c</sup>
VAWC-1	-14.7	9.2	0.7	29.2	29.9	
$B_{AC}2-1$	-20.2	2.8	-5.7	30.7	24.9	24.6 [10.9]
$B_{AL}2-1$	-7.3	14.8	6.3	28.9	35.1	

<sup>a</sup>Relative free energy after adjustment for the concentration in the liquid,  $p = 1354$  atm. <sup>b</sup> $\Delta G_{\text{aq}} = \Delta G + \Delta \Delta G_{\text{solv}}$ . <sup>c</sup>Experimental values from ref 12.

According to the SMD-M06/B4//B3LYP/B2 calculations, the activation energy decreases by 5 kcal/mol on going from  $B_{AL}2-1$  to VAWC-1 and by the same amount from VAWC-1 to  $B_{AC}2-1$ . All levels of theory point to  $B_{AC}2-1$  as the most probable reaction mechanism for pNPA hydrolysis catalyzed by the H<sub>2</sub>VO<sub>4</sub><sup>-</sup> ion in aqueous media. This result is in agreement with the experimental data,<sup>12</sup> suggesting nucleophilic addition in the rate-limiting transition state and the formation of a tetrahedral intermediate. Moreover, the  $B_{AC}2-1$  rate-limiting barrier height

(−24.9 kcal/mol) obtained from SMD-M06/B4//B3LYP/B2 is in excellent agreement with the experimentally estimated activation Gibbs function for vanadate-promoted pNPA hydrolysis (−24.6 kcal/mol).<sup>12</sup> The molecular arrangement in TS1 of B<sub>AC</sub>2-1 is in line with the observed solvent deuterium isotope effect of 1.27. Values higher than about 1.5 are interpreted as an indication of a proton in flight in the transition state of the rate-limiting step, pointing to a general base mechanism. Unlike previous suggestions,<sup>12</sup> the tetrahedral intermediate of the B<sub>AC</sub>2-1 pathway is stabilized through protonation of the negatively charged acyl oxygen atom and the formation of a V–O⋯HO–C(acyl) hydrogen bond rather than through coordination of the acyl oxygen atom to vanadium [like the proposed mechanism of the MO<sub>4</sub><sup>2−</sup> (M = Mo, Cr) catalyzed ester hydrolysis], giving rise to a chelate complex. According to our calculations, the energy gained from protonation of the adduct with the formation of a six-membered hydrogen-bonded ring is much more pronounced than that gained from the formation of a strained four-membered chelate ring, as is the case in the INT structures of the B<sub>AC</sub>2-3 and B<sub>AC</sub>2-4 pathways (Figures S5 and S6 in the SI). For instance, the SMD-M06/B4//B3LYP/B2 energy of the INT structure in B<sub>AC</sub>2-1 is around 10 kcal/mol lower than the energies of the corresponding INT chelate structures in B<sub>AC</sub>2-3 and B<sub>AC</sub>2-4. However, in the case of MO<sub>4</sub><sup>2−</sup> (M = Cr, Mo)-catalyzed reactions of hydrolysis, where the formation of such hydrogen-bonded intermediates is not expected (at neutral pH, chromate and molybdate exist mainly in their deprotonated forms), INT stabilization via formation of a chelate complex might still be plausible.

Vanadium(V) exhibits a rich aqueous chemistry, the detected species of which are strongly dependent upon the pH and vanadium concentration. Indeed, this system is characterized by numerous equilibria associated with hydrolysis and polymerization reactions where various mono- and polynuclear entities are involved.<sup>7</sup> Although it was confirmed by experiment that, under the reaction conditions of pNPA hydrolysis, divanadate, tetravanadate, and pentavanadate are also present, kinetic evidence points toward monovanadate as the catalytically active species.<sup>12</sup> The question why the catalytic activity is expressed by monovanadate, rather than by, e.g., divanadate or tetravanadate, remains open and will be addressed in further investigations. Most probably, the underlying reasons should be sought either in the possibility for favorable molecular arrangements in the rate-limiting transition state and the subsequent INT or in different solvation effects. Because they exist mainly in their deprotonated forms, tetravanadate and pentavanadate possess high negative charges (4− and 5−, respectively). As such, the formation of molecular structures analogous to TS1 and INT in the B<sub>AC</sub>2-1 mechanism, where the role of (VO−)H protons is essential, is less feasible. On the other hand, divanadate is less bulky, and the commonly accepted structure of this ion does contain two (V−)OH groups that could interact with pNPA in the same way as monovanadate. Because both monovanadate and divanadate are present in similar concentrations in the reaction mixture, other factors (steric, electronic, etc.) should account for the experimentally suggested catalytic activity of monovanadate rather than that of divanadate. A possible explanation could be found on the basis of solvation effects. Considering the higher negative charge of divanadate (2−) and, of course, even more so for tetravanadate (4−) or pentavanadate (5−), more extensive solvation of these species may be expected and,

hence, the partial removal of solvent molecules involves more solvent reorganization than is the case for monovanadate.

## CONCLUSIONS

This work deals with the mechanisms of *p*-nitrophenyl acetate ester bond cleavage catalyzed by the monovanadate ion in aqueous solution. To study this catalytic reaction, a number of DFT and ab initio methods were utilized. Four possible B<sub>AC</sub>2 mode reaction pathways were modeled, in line with the experimental evidence. In addition, two alternative reaction modes, VAWC and B<sub>AL</sub>2, were also considered. Geometry optimizations were performed with three different DFTs, and single-point energy calculations were performed at 15 levels of theory. Solvation effects were accounted for by means of SMD and CPCM solvation models. From the obtained results, the following conclusions can be drawn.

pNPA hydrolysis catalyzed by the monovanadate ion in aqueous media most likely proceeds as a two-step mechanism: the first step is associated with the nucleophilic addition of the vanadate ion to the acyl carbon atom, and the second step is associated with the release of the leaving group (the B<sub>AC</sub>2-1 mechanism). This result is in agreement with the experiment, suggesting a nucleophilic addition in the rate-limiting transition state with the formation of a tetrahedral intermediate. The theoretically predicted intermediate structure is stabilized through protonation of the negatively charged acyl oxygen atom (by the vanadate) and the formation of a V–O⋯HO–C(acyl) hydrogen bond rather than through coordination of the acyl oxygen atom to the vanadium atom and formation of a chelate complex. The energy gain obtained from protonation of the adduct with the formation of a six-membered hydrogen-bonded ring is much more pronounced compared to the formation of a strained four-membered chelate ring. A comparison of the calculated activation energies unambiguously shows that, as could be expected, the B<sub>AL</sub>2 reaction modes are less likely than the B<sub>AC</sub>2 and VAWC modes. The B<sub>AC</sub>2-1, VAWC-1, and B<sub>AL</sub>2-1 mechanisms were found as the lowest-energy pathways on the PES for the corresponding reaction modes. With respect to B<sub>AC</sub>2-1, the activation energies of the VAWC-1 and B<sub>AL</sub>2-1 pathways are calculated to be higher by 5 and 10 kcal/mol, respectively. For the stepwise mechanisms of both the B<sub>AC</sub>2 and VAWC modes, the first addition step has the highest energy requirement and is the bottleneck for the overall process. Excellent agreement between the calculated rate-limiting barrier height of the B<sub>AC</sub>2-1 mechanism and the experimental activation energy for vanadate-promoted pNPA hydrolysis was obtained with the M06 functional, followed by B3LYP-D and B2PLYP-D methods, combined with B4 basis sets and the SMD solvation model.

To the best of our knowledge, this is the first theoretical work that sheds light on the catalytic activity of oxovanadate ions toward carboxylic acid ester hydrolysis in solution. The present results may serve as a useful guide for understanding the mechanism of other analogous reactions involving vanadate and may contribute to a better understanding of its biological role.

## ASSOCIATED CONTENT

### Supporting Information

Description of the VAWC-2, VAWC-3, B<sub>AC</sub>2-2, B<sub>AC</sub>2-3, B<sub>AC</sub>2-4, and B<sub>AL</sub>2-2 mechanisms, thermodynamic data of all species along the reaction pathways calculated at different levels of theory, a discussion entitled “Comparison of the methods”, and



optimized geometries of all species along the reaction pathways in Cartesian coordinates. This material is available free of charge via the Internet at <http://pubs.acs.org>.

## AUTHOR INFORMATION

### Corresponding Author

\*E-mail: [tzmihay@svr.igic.bas.bg](mailto:tzmihay@svr.igic.bas.bg).

### Notes

The authors declare no competing financial interest.

## ACKNOWLEDGMENTS

This investigation has been supported by grants from the Flemish Science Foundation and from the Concerted Research Action of the Flemish Government (GOA). T.M. thanks KU Leuven for financial support under a BOF-F+ contract connected to the GOA "Multicentre Quantum Chemistry" project.

## REFERENCES

- (1) Chasteen, N. D. *Vanadium in biological systems: physiology and biochemistry*; Kluwer Academic Publishers: Dordrecht, The Netherlands, 1990.
- (2) Shechter, Y.; Karlish, S. J. D. *Nature* **1980**, *284*, 556–558.
- (3) Heyliger, C. E.; Tahiliani, A. G.; McNeill, J. H. *Science* **1985**, *1474*–1477.
- (4) Reul, B. A.; Amin, S. S.; Buchet, J.-P.; Ongemba, L. N.; Crans, D. C.; Brichard, S. M. *Br. J. Pharmacol.* **1999**, *126*, 467–477.
- (5) Aureliano, M.; Crans, D. C. *J. Inorg. Biochem.* **2009**, *103*, 536–546.
- (6) Aureliano, M. *Dalton Trans.* **2009**, 9093–9100.
- (7) Crans, D. C.; Smees, J. J.; Gaidamauskas, E.; Yang, L. *Chem. Rev.* **2004**, *104*, 849–902.
- (8) Crans, D. C. *Pure Appl. Chem.* **2005**, *77*, 1497–1527.
- (9) Rehder, D. In *Bioinorganic Vanadium Chemistry*; John Wiley & Sons: New York, 2008; pp 158–201.
- (10) Steens, N.; Ramadan, A. M.; Parac-Vogt, T. N. *Chem. Commun.* **2009**, *28*, 965–967.
- (11) Steens, N.; Ramadan, A. M.; Absillis, G.; Parac-Vogt, T. N. *Dalton Trans.* **2010**, *39*, 585–592.
- (12) Ho, P. H.; Breyneert, E.; Kirschhock, C. E. A.; Parac-Vogt, T. N. *Dalton Trans.* **2011**, *40*, 295–300.
- (13) Williams, A. *Acc. Chem. Res.* **1989**, *22*, 387–392.
- (14) Cleland, W. W.; Hengge, A. C. *FASEB J.* **1995**, *9*, 1585–1594.
- (15) Takashima, K.; Jose, S. M.; do Amaral, A. T.; Riveros, J. M. *J. Chem. Soc., Chem. Commun.* **1983**, 1255–1256.
- (16) Ba-Saif, S. A.; Luthra, A. K.; Williams, A. *J. Am. Chem. Soc.* **1987**, *109*, 6362–6368.
- (17) Ba-Saif, S. A.; Luthra, A. K.; Williams, A. *J. Am. Chem. Soc.* **1989**, *111*, 2647–2652.
- (18) Ba-Saif, S. A.; Waring, M. A.; Williams, A. *J. Am. Chem. Soc.* **1990**, *112*, 8115–8120.
- (19) Guthrie, J. P. *J. Am. Chem. Soc.* **1991**, *113*, 3941–3949.
- (20) Hengge, A. *J. Am. Chem. Soc.* **1992**, *114*, 6575–6576.
- (21) Gellman, S. H.; Petter, R.; Breslow, R. *J. Am. Chem. Soc.* **1986**, *108*, 2388–2394.
- (22) Koike, T.; Kimura, E. *J. Am. Chem. Soc.* **1991**, *113*, 8935–8941.
- (23) Kimura, E. *Tetrahedron* **1992**, *48*, 6175–6217.
- (24) Kimura, E.; Koike, T. *Chem. Commun.* **1998**, 1495–1599.
- (25) Looney, A.; Parkin, G.; Alsfasser, R.; Ruf, M.; Vahrenkamp, H. *Angew. Chem., Int. Ed. Engl.* **1992**, *31*, 92–93.
- (26) Ruf, M.; Weis, K.; Vahrenkamp, H. *J. Am. Chem. Soc.* **1996**, *118*, 9288–9294.
- (27) Hikichi, S.; Tanaka, M.; Moro-oka, Y.; Kitajima, N. *J. Chem. Soc., Chem. Commun.* **1992**, 814–815.
- (28) Altava, B.; Burguete, M. L.; Luis, S. V.; Miravet, J. F.; Garcia-España, E.; Marcelino, V.; Soriano, C. *Tetrahedron* **1997**, *57*, 4751–4762.
- (29) Sigel, H. *Coord. Chem. Rev.* **1990**, *100*, 453–539.
- (30) Chin, J. *Acc. Chem. Res.* **1991**, *24*, 145–152.
- (31) Chadhuri, P.; Atockneim, C.; Wieghardt, K.; Deck, W.; Gregorzic, R.; Vahrenkamp, H.; Nuber, B.; Weiss, J. *Inorg. Chem.* **1992**, *31*, 1451–1457.
- (32) Williams, I. H.; Spangler, D.; Femec, D. A.; Maggiora, G. M.; Schowen, R. L. *J. Am. Chem. Soc.* **1983**, *105*, 31–40.
- (33) Sherer, E. C.; Turner, G. M.; Shields, G. C. *Int. J. Quantum Chem. Quantum Biol. Symp.* **1995**, *22*, 83–93.
- (34) Turner, G. M.; Sherer, E. C.; Shields, G. C. *Int. J. Quantum Chem. Quantum Biol. Symp.* **1995**, *22*, 103–112.
- (35) Sherer, E. C.; Yang, G.; Turner, G. M.; Shields, G. C.; Landry, D. W. *J. Phys. Chem. A* **1997**, *101*, 8526–8529.
- (36) Zhan, C.-G.; Landry, D. W.; Ornstein, R. L. *J. Am. Chem. Soc.* **2000**, *122*, 1522–1533.
- (37) Zhan, C.-G.; Landry, D. W.; Ornstein, R. L. *J. Am. Chem. Soc.* **2000**, *122*, 2621–2627.
- (38) Zhan, C.-G.; Landry, D. W.; Ornstein, R. L. *J. Phys. Chem. A* **2000**, *104*, 7672–7678.
- (39) Bender, M. L.; Turnquest, B. W. *J. Am. Chem. Soc.* **1957**, *79*, 1652–1655.
- (40) Sacher, E.; Laidler, K. J. *Can. J. Chem.* **1964**, *42*, 2404–2409.
- (41) Fallerand, L.; Sturevant, J. M. *J. Biol. Chem.* **1966**, *241*, 4825–4834.
- (42) Rawlings, J.; Cleland, W. W.; Hengge, A. C. *J. Inorg. Biochem.* **2003**, *93*, 61–65.
- (43) Johnson, S. L. *J. Am. Chem. Soc.* **1962**, *84*, 1729–1734.
- (44) Hess, R. A.; Hengge, A. C.; Cleland, W. W. *J. Am. Chem. Soc.* **1997**, *119*, 6980–6983.
- (45) Wikjord, B.; Byers, L. D. *J. Am. Chem. Soc.* **1992**, *114*, 5553–5554.
- (46) Wikjord, B. R.; Byers, L. D. *J. Org. Chem.* **1992**, *57*, 6814–6817.
- (47) Ahn, B.-T.; Park, H.-S.; Lee, E.-J.; Um, I.-H. *Bull. Korean Chem. Soc.* **2000**, *21*, 905–908.
- (48) Becke, A. D. *J. Chem. Phys.* **1993**, *98*, 5648–5652.
- (49) Lee, C.; Yang, W.; Parr, R. G. *Phys. Rev. B* **1988**, *37*, 785–789.
- (50) Stevens, P. J.; Devlin, F. J.; Chabalowski, C. F.; Frish, M. J. *J. Phys. Chem.* **1994**, *98*, 11623–11627.
- (51) Hay, P. J.; Wadt, W. R. *J. Chem. Phys.* **1985**, *82*, 270–283.
- (52) Hay, P. J.; Wadt, W. R. *J. Chem. Phys.* **1985**, *82*, 299–310.
- (53) Dolg, M.; Wedig, U.; Stoll, H.; Preuss, H. *J. Chem. Phys.* **1987**, *86*, 866–872.
- (54) Xu, X.; Alecu, I. M.; Truhlar, D. G. *J. Chem. Theory Comput.* **2011**, *7*, 1667–1676.
- (55) Becke, A. D. *J. Chem. Phys.* **1996**, *104*, 1040–1046.
- (56) Zhao, Y.; Truhlar, D. G. *J. Phys. Chem. A* **2004**, *108*, 6908–6918.
- (57) Zhao, Y.; Gonzales-Garcia, N.; Truhlar, D. G. *J. Phys. Chem. A* **2005**, *109*, 2012–2018.
- (58) Ribeiro, A. J. M.; Ramos, M. J.; Fernandes, P. A. *J. Chem. Theory Comput.* **2010**, *6*, 2281–2292.
- (59) Zhao, Y.; Truhlar, D. G. *Theor. Chem. Acc.* **2008**, *120*, 215–241.
- (60) Zhao, Y.; Truhlar, D. G. *Acc. Chem. Res.* **2008**, *41*, 157–167.
- (61) Zhao, Y.; Pu, J.; Lynch, B. J.; Truhlar, D. G. *J. Phys. Chem. Chem. Phys.* **2004**, *6*, 673–676.
- (62) Grimme, S. *J. Chem. Phys.* **2006**, *124*, 034108–16.
- (63) Schwabe, T.; Grimme, S. *J. Phys. Chem. Chem. Phys.* **2007**, *9*, 3397–3406.
- (64) Goerigk, L.; Grimme, S. *J. Chem. Theory Comput.* **2010**, *6*, 107–126.
- (65) Marenich, A. V.; Cramer, C. J.; Truhlar, D. G. *J. Phys. Chem. B* **2009**, *113*, 6378–6396.
- (66) Barone, V.; Cossi, M. *J. Phys. Chem. A* **1998**, *102*, 1995–2001.
- (67) Cossi, M.; Rega, N.; Scalmani, G.; Barone, V. *J. Comput. Chem.* **2003**, *24*, 669–681.
- (68) Takano, Y.; Houk, K. N. *J. Chem. Theory Comput.* **2005**, *1*, 70–77.
- (69) Strajbl, M.; Sham, Y. Y.; Villa, J.; Chu, Z.-T.; Warshel, A. *J. Phys. Chem. B* **2000**, *104*, 4578–4584.
- (70) Ben-Naim, A.; Marcus, Y. *J. Chem. Phys.* **1984**, *81*, 2016–2028.

(71) Jalan, A.; Ashcraft, R. W.; West, R. H.; Green, W. H. *Annu. Rep. Prog. Chem., Sect. C* **2010**, *106*, 211–258.

(72) Ho, J.; Klamt, A.; Coote, M. L. *J. Phys. Chem. A* **2010**, *114*, 13442–13444.

(73) Martin, R. L.; Hay, P. J.; Pratt, L. R. *J. Phys. Chem. A* **1998**, *102*, 3565–3573.

(74) Frisch, M. J.; Trucks, G. W.; Schlegel, H. B.; Scuseria, G. E.; Robb, M. A.; Cheeseman, J. R.; Montgomery, J. A., Jr.; Vreven, T.; Kudin, K. N.; Burant, J. C.; Millam, J. M.; Iyengar, S. S.; Tomasi, J.; Barone, V.; Mennucci, B.; Cossi, M.; Scalmani, G.; Rega, N.; Petersson, G. A.; Nakatsuji, H.; Hada, M.; Ehara, M.; Toyota, K.; Fukuda, R.; Hasegawa, J.; Ishida, M.; Nakajima, T.; Honda, Y.; Kitao, O.; Nakai, H.; Klene, M.; Li, X.; Knox, J. E.; Hratchian, H. P.; Cross, J. B.; Bakken, V.; Adamo, C.; Jaramillo, J.; Gomperts, R.; Stratmann, R. E.; Yazyev, O.; Austin, A. J.; Cammi, R.; Pomelli, C.; Ochterski, J. W.; Ayala, P. Y.; Morokuma, K.; Voth, G. A.; Salvador, P.; Dannenberg, J. J.; Zakrzewski, V. G.; Dapprich, S.; Daniels, A. D.; Strain, M. C.; Farkas, O.; Malick, D. K.; Rabuck, A. D.; Raghavachari, K.; Foresman, J. B.; Ortiz, J. V.; Cui, Q.; Baboul, A. G.; Clifford, S.; Cioslowski, J.; Stefanov, B. B.; Liu, G.; Liashenko, A.; Piskorz, P.; Komaromi, I.; Martin, R. L.; Fox, D. J.; Keith, T.; Al-Laham, M. A.; Peng, C. Y.; Nanayakkara, A.; Challacombe, M.; Gill, P. M. W.; Johnson, B.; Chen, W.; Wong, M. W.; Gonzalez, C.; Pople, J. A. *Gaussian 03*, revision E.01; Gaussian, Inc.: Wallingford, CT, 2004.

(75) Frisch, M. J.; Trucks, G. W.; Schlegel, H. B.; Scuseria, G. E.; Robb, M. A.; Cheeseman, J. R.; Scalmani, G.; Barone, V.; Mennucci, B.; Petersson, G. A.; Nakatsuji, H.; Caricato, M.; Li, X.; Hratchian, H. P.; Izmaylov, A. F.; Bloino, J.; Zheng, G.; Sonnenberg, J. L.; Hada, M.; Ehara, M.; Toyota, K.; Fukuda, R.; Hasegawa, J.; Ishida, M.; Nakajima, T.; Honda, Y.; Kitao, O.; Nakai, H.; Vreven, T.; Montgomery, J. A., Jr.; Peralta, J. E.; Ogliaro, F.; Bearpark, M.; Heyd, J. J.; Brothers, E.; Kudin, K. N.; Staroverov, V. N.; Kobayashi, R.; Normand, J.; Raghavachari, K.; Rendell, A.; Burant, J. C.; Iyengar, S. S.; Tomasi, J.; Cossi, M.; Rega, N.; Millam, J. M.; Klene, M.; Knox, J. E.; Cross, J. B.; Bakken, V.; Adamo, C.; Jaramillo, J.; Gomperts, R.; Stratmann, R. E.; Yazyev, O.; Austin, A. J.; Cammi, R.; Pomelli, C.; Ochterski, J. W.; Martin, R. L.; Morokuma, K.; Zakrzewski, V. G.; Voth, G. A.; Salvador, P.; Dannenberg, J. J.; Dapprich, S.; Daniels, A. D.; Farkas, O.; Foresman, J. B.; Ortiz, J. V.; Cioslowski, J.; Fox, D. J. *Gaussian 09*, revision A.02; Gaussian, Inc.: Wallingford, CT, 2009.

(76) Lowry, T. H.; Richardson, K. S. *Mechanism and Theory in Organic Chemistry*; Harper and Row: New York, 1987.

(77) Hengge, A. C.; Hess, R. A. *J. Am. Chem. Soc.* **1994**, *116*, 11256–11263.

(78) Tantillo, D. J.; Houk, K. N. *J. Org. Chem.* **1999**, *64*, 3066–3076.

(79) Bühl, M.; Parrinello, M. *Chem.—Eur. J.* **2001**, *7*, 4487–4494.

(80) Sadoc, A.; Messaoudi, S.; Futet, E.; Gautier, R.; Fur, E. L.; le Polles, L.; Pivan, J.-Y. *Inorg. Chem.* **2007**, *46*, 4835–4843.

(81) Tracey, A. S.; Li, H.; Grasser, M. J. *Inorg. Chem.* **1990**, *29*, 2267–2271.

(82) Galeffi, B.; Tracey, A. S. *Can. J. Chem.* **1988**, *66*, 2565–2569.

(83) Sirotkin, V. A.; Huettl, R.; Wolf, G. *Thermochim. Acta* **2005**, *426*, 1–6.

(84) Tracey, A. S.; Willsky, G. R.; Takeuchi, E. S. *Vanadium Chemistry, Biochemistry, Pharmacology and Practical Applications*; CRC Press: Boca Raton, FL, 2007.